International Journal of Sustainable Aviation

ISSN online: 2050-0475 - ISSN print: 2050-0467
https://www.inderscience.com/ijsa

Performing trajectory tracking control of an unmanned ground vehicle using fractional order terminal sliding mode controller

Hayriye Tuğba Sekban, Abdullah Başçi

DOI: 10.1504/IJSA.2023.10051829

Article History:

Received:	28 December 2021
Accepted:	07 June 2022
Published online:	06 December 2022

Performing trajectory tracking control of an unmanned ground vehicle using fractional order terminal sliding mode controller

Hayriye Tuğba Sekban

Department of Electronics and Automation,
Bayburt University,
Bayburt, Turkey
Email: tugbasekban@bayburt.edu.tr

Abdullah Başçi*

Department of Electrical and Electronics Engineering,
Ataturk University,
Erzurum, Turkey
Email: abasci@atauni.edu.tr
*Corresponding author

Abstract: In this paper, fractional order terminal sliding mode control (FOTSMC) method is used for trajectory tracking control performance of an unmanned ground vehicle (UGV). Firstly, a kinematic controller is designed to estimate the linear and angular velocities of the vehicle. Then, a FOTSMC design is carried out to track the vehicle reference velocities. Terminal sliding mode control (TSMC) and sliding mode control (SMC) methods are also used to demonstrate the performance of the proposed controller. The simulation results show that the proposed controller improves the tracking error by about 13% over SMC and 6.146% compared to TSMC.

Keywords: unmanned ground vehicle; UGV; trajectory tracking control; kinematic control; fractional order terminal sliding mode control.

Reference to this paper should be made as follows: Sekban, H.T. and Başçi, A. (2023) 'Performing trajectory tracking control of an unmanned ground vehicle using fractional order terminal sliding mode controller', *Int. J. Sustainable Aviation*, Vol. 9, No. 1, pp.73–88.

Biographical notes: Hayriye Tuğba Sekban received his BS and MS in Electrical and Electronics Engineering at the Atatürk University, Turkey in 2013 and 2017, respectively. She is currently a Lecturer at the Bayburt University. Her research interests focus on unmanned ground vehicles, robotic systems, control systems, sliding mode control, and fractional control.

Abdullah Başçi received his BS in Electrical Engineering from the Pamukkale University, Turkey in 2004, and MS form the University of East London, London, UK in 2008. He is currently an Associate Professor in Electrical and Electronics Engineering at the Atatürk University. His research interests include control of wheeled mobile robot, electrical machines, sensorless control of IMs, fuzzy and sliding mode control techniques.

This paper is a revised and expanded version of a paper entitled 'Trajectory tracking control of an unmanned ground vehicle based on fractional order terminal sliding mode controller' presented at ISUDEF, Howard University, Washington DC, USA, 26–28 October 2021.

1 Introduction

Unmanned ground vehicles (UGV) are a type of non-holonomic mechanical systems and are divided into several groups as wheeled ground vehicles, legged ground vehicles and tracked ground vehicles. Wheeled ground vehicles are often preferred in real applications such as transport, mine clearance and carrying passengers luggage in airport terminals due to their many advantages such as high energy efficiency, good stability, fast motion and low mechanical complexity. Because the difficulties in implementation, uncertainties and non-holonomic constraints many researchers have focused on vehicle trajectory tracking control (Mevo et al., 2018). Trajectory control, both requires the controller design for the vehicle to follow a determined trajectory and must stabilise the closed-loop system robustly against system uncertainties (Xin et al., 2016). In recent years, studies have been dealing with kinematic tracking problems without considering the UGV dynamics. However, taking into account only a kinematic model in a real trajectory problem is inadequate to achieve good tracking performance due to vehicle dynamics, such as high speed or carrying heavy load (Başçi et al., 2015). Therefore, the combined use of both kinematic and dynamic models in trajectory tracking of UGVs provides more realistic results (Koubaa et al., 2015).

PID controllers have been the most popular and widely used industrial controllers in recent years. The popularity and widespread use of PID controllers is primarily attributed to their simple construction, reliability, easy parameters adjust, good performance and not dependence on the precise dynamic mathematical model of the system they control. Linear fixed-gain PID controllers are tuned to operate based on system behaviour in a certain limited operating region. If a system's behaviour and/or operating region changes over time, the PID controller will need to be readjusted to function as intended. An original combination of standard PID and kinematic based backstepping controllers has been developed for a differential drive mobile robot to be able to track a desired trajectory (Demirbas and Kalyoncu, 2017). Here, with the simplest nonlinear kinematic model, a backstepping controller was used to overcome the nonlinearity of the trajectory tracking and the PID controllers were applied for the DC motors' speeds adjustments by the error signals. The responses of the developed simple controller were obtained with a significant reduction in the settling time and overshot.

Nonlinear control methods such as fuzzy control, backstepping method, finite time control, neural network control and sliding mode control (SMC) are used to overcome the poor control performance encountered in the application of fixed parameter linear controllers to nonlinear or time-varying systems (Başçi and Derdiyok, 2014; Fierro and Lewis, 1997; Ou et al., 2014; Ding et al., 2020; Orman et al., 2018). SMC is one of the most effective control methods widely preferred to achieve trajectory tracking control of non-holonomic UGV due to its strong robustness against model uncertainties, disturbances, good transient performance and very easy design (Young et al., 1996; Asif et al., 2014; Sharma and Panwar, 2016; Sekban and Başçi, 2021). The biggest

disadvantages of the SMC controller are the chattering in the systems and the reaches asymptotic stability in infinite time. Various methods such as filtering, discontinuous approximation, fuzzy control and high-order sliding mode controller are used to reduce the chattering effect (Başçi and Derdiyok, 2013). The problem of asymptotic convergence of system states in infinite time is solved by using a terminal sliding mode controller (TSMC) (Yu et al., 2020; Sekban et al., 2021).

With the developing technology, the interest in fractional order calculus has increased rapidly. Fractional order calculation plays an important role in many fields such as control engineering, viscoelastic fluids, physics, power converters, mechatronic systems, signal processing and its applied fields is increasing day by day (Sekban et al., 2020; Çelebi and Başçi, 2016; Can et al., 2020a). In recent years, studies on fractional order systems have been pioneers for control engineering applications. Studies have shown that fractional differential equations are an effective tool for describing complex equations and also an effective method for modelling many systems (Oustaloup et al., 2000). To take advantage of these advantages of fractional order calculus, various controllers such as the fractional order PID controller, the fractional order SMC and the fractional order adaptive controller have been developed one after the other (Orman et al., 2016; Can et al., 2020b).

In this paper, fractional order terminal sliding mode control (FOTSMC), TSMC and SMC are used to perform trajectory tracking control of UGV under different linear and angular velocity references. Numerical simulation results demonstrate the efficiency and robustness of FOTSMC than to TSMC and SMC.

2 Material and method

Many parameters are taken into account for the number and arrangement of wheels to be used in the vehicle. However, the most important issues to be considered are the control mechanism of the wheels and the mechanical moment to be obtained. In this study, a non-holonomic UGV with one caster wheel at the front and two differential driving wheels at the rear is discussed. Many researchers have shown that this configuration is sufficient to stabilise the vehicle. The caster wheel at the front of the UGV is used to keep the vehicle in balance and reduce the load on the rear wheels. On the other hand, the rear differential driving wheels, are connected to independently controlled motors and provide the vehicle to change direction by moving the vehicle backward and forward. Thus, there is no need to use a separate motor for routing. This both reduces the cost and enables the size to be reduced. The illustration of the mentioned non-holonomic UGV is shown in Figure 1.

In Figure 1, x_I, y_I is the global axis, x_r, y_r is the local axis, x_A, y_A is the coordinate components with respect to point A, A is the midpoint of the two wheels, C is the centre of gravity of the vehicle, r is the radius of the each used wheel, L is the distance of each wheel to point A, v is the linear velocity of vehicle, ω is the angular velocity of the vehicle, ω_R and ω_L are the angular velocity of the right and left wheel respectively, θ is the angle between the local and global axis and d is the distance between point A and C.

To determine the position of UGV in its environment, two different coordinate axes called global axis (q^I) and local axis (q^r) are used and the transformation between the axes

is provided by the rotation matrix ($R(\theta)$). These expressions are as specified in equation (1).

$$q^I = \begin{bmatrix} x^I \\ y^I \\ \theta^I \end{bmatrix}, q^r = \begin{bmatrix} x^r \\ y^r \\ \theta^r \end{bmatrix}, R(\theta) = \begin{bmatrix} \cos\theta & -\sin\theta & 0 \\ \sin\theta & \cos\theta & 0 \\ 0 & 0 & 1 \end{bmatrix} \tag{1}$$

Figure 1 Schematics of UGV

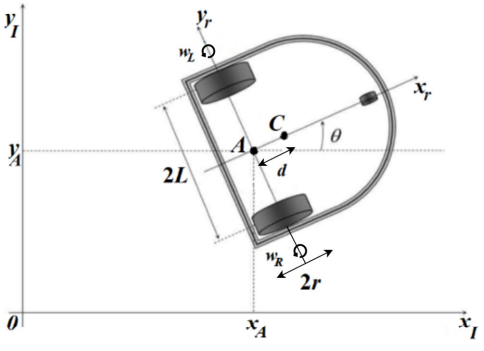

3 Modelling of UGV

Analysis of UGV's mathematical model is the basis for controller design and obtaining a precise mathematical model is crucial to controller performance. The mathematical model of UGV is divided into kinematic and dynamic model.

3.1 Kinematic model of UGV

The purpose of kinematic modelling is to describe the relationship between the linear and angular velocity, position and angle of the UGV (Wang et al., 2020). The kinematic model of the UGV with the assumption that the wheel rolls without slipping and without pivoting on the ground constraints is as follows (Azzabi and Nouri, 2021).

$$\dot{q}^I = \begin{bmatrix} \dot{x}_A^I \\ \dot{y}_A^I \\ \dot{\theta}_A^I \end{bmatrix} = \begin{bmatrix} \cos\theta & 0 \\ \sin\theta & 0 \\ 0 & 1 \end{bmatrix} \begin{bmatrix} v \\ \omega \end{bmatrix} = S(q)\eta \tag{2}$$

The mathematical expression of the linear and angular velocities of the UGV can be expressed as a function of the linear and angular velocities of the left wheel and the right wheel and are calculated as follows.

$$v = (v_R + v_L)/2 = r(\omega_R + \omega_L)/2 \tag{3}$$

$$\omega = (v_R - v_L)/2L = r(\omega_R - \omega_L)/2L \tag{4}$$

The velocities of point A with according to the global coordinate axis are obtained in terms of the angular velocities of the right and left wheels by using the orthogonal rotation matrix as given below.

$$\dot{q}^I = \begin{bmatrix} \dot{x}_A^I \\ \dot{y}_A^I \\ \dot{\theta}_A^I \end{bmatrix} = \begin{bmatrix} \frac{r}{2}\cos\theta & \frac{r}{2}\cos\theta \\ \frac{r}{2}\sin\theta & \frac{r}{2}\sin\theta \\ \frac{r}{2L} & -\frac{r}{2L} \end{bmatrix} \begin{bmatrix} \omega_R \\ \omega_L \end{bmatrix} \tag{5}$$

3.2 Dynamic model of UGV

The aim of the dynamic model is to express the relationship between linear and angular velocities, linear and angular acceleration of UGV motion (Wang et al., 2020). The dynamic equation of non-holonomic UGV is described as follows (Swadi et al., 2016).

$$M(q)\ddot{q} + V(q,\dot{q})\dot{q} + F(\dot{q}) + G(q) + \tau_d = B(q)\tau - A^T(q)\lambda \tag{6}$$

$M(q)$ is the symmetric positive definite inertia matrix, $V(q,\dot{q})$ is the centripetal and coriolis matrix, $F(\dot{q})$ is the surface friction matrix, $G(q)$ is the gravitational vector τ_d is the vector of bounded unknown disturbances including unstructured unmodelled dynamics, $B(q)$ is the input matrix, τ is the input vector, $A(q)$ is the matrix associated with the kinematic constraints, λ is the Lagrange multipliers vector, q, $\dot{q}$ and $\ddot{q}$ denote position, velocity and acceleration vectors respectively.

Assuming that vehicle moves in a horizontal plane and there is no surface friction, gravity and disturbance (Azzabi and Nouri, 2021). The resulting new equation is as follows.

$$M(q)\ddot{q} + V(q,\dot{q})\dot{q} = B(q)\tau - A^T(q)\lambda \tag{7}$$

For this, equation (2) and its derivative are obtained as follows.

$$\left.\begin{aligned} \dot{q} &= S(q)\eta \\ \ddot{q} &= \dot{S}(q)\eta + S(q)\dot{\eta} \end{aligned}\right\} \tag{8}$$

If equation (8) is substituted in equation (7) the following equation is obtained.

$$M(q)\left[\dot{S}(q)\eta + S(q)\dot{\eta}\right] + V(q,\dot{q})\left[S(q)\eta\right] = B(q)\tau - A^T(q)\lambda \tag{9}$$

Equation (9) in $S(q)$ matrix is the null space of the $A(q)$ matrix such that is given below.

$$A(q)^T S(q)^T = 0 \tag{10}$$

The dynamic equation of UGV, arranged by multiplying both sides of the equation (9) by $S(q)^T$ is obtained as follows (Chen et al., 2009).

$$\tilde{M}(q)\dot{\eta} + \tilde{V}(q,\dot{q})\eta = \tilde{B}(q)\tau \tag{11}$$

$\tilde{M}(q), \tilde{V}(q,\dot{q})$ and $\tilde{B}(q)$ are obtained by using the following equations.

$$\left.\begin{array}{c} \tilde{M}(q) = S(q)^T M(q) S(q) \\ \tilde{V}(q,\dot{q}) = S(q)^T M(q)\dot{S}(q) + S(q)^T V(q,\dot{q}) S(q) \\ \tilde{B}(q) = S(q)^T B(q) \end{array}\right\} \tag{12}$$

The $\tilde{M}(q), \tilde{V}(q,\dot{q})$ and $\tilde{B}(q)$ matrices in equation (12) are obtained as follows,

$$\begin{aligned} \tilde{M}(q) &= \begin{bmatrix} I_w + \frac{r^2}{4L^2}(mL^2 + I) & \frac{r^2}{4L^2}(mL^2 - I) \\ \frac{r^2}{4L^2}(mL^2 - I) & I_w + \frac{r^2}{4L^2}(mL^2 + I) \end{bmatrix} \\ \tilde{V}(q,\dot{q}) &= \begin{bmatrix} 0 & \frac{r^2}{2L} m_c d\dot{\theta} \\ -\frac{r^2}{2L} m_c d\dot{\theta} & 0 \end{bmatrix} \\ \tilde{B}(q) &= \begin{bmatrix} 1 & 0 \\ 0 & 1 \end{bmatrix} \end{aligned} \tag{13}$$

where I is the total equivalent inertia, I_w is the moment of inertia of each driving wheel with a motor about the wheel axis, m is the total mass of the UGV, m_c is the UGV mass without driving wheels and actuators. If the matrices in equation (13) are substituted in equation (11), the dynamic equation of UGV is obtained as follows.

$$\begin{aligned} &\begin{bmatrix} I_w + \frac{r^2}{4L^2}(mL^2 + I) & \frac{r^2}{4L^2}(mL^2 - I) \\ \frac{r^2}{4L^2}(mL^2 - I) & I_w + \frac{r^2}{4L^2}(mL^2 + I) \end{bmatrix} \dot{\eta} + \begin{bmatrix} 0 & \frac{r^2}{2L} m_c d\dot{\theta} \\ -\frac{r^2}{2L} m_c d\dot{\theta} & 0 \end{bmatrix} \eta \\ &= \begin{bmatrix} 1 & 0 \\ 0 & 1 \end{bmatrix} \begin{bmatrix} \tau_R \\ \tau_L \end{bmatrix} \end{aligned} \tag{14}$$

Using equation (3) and (4), the equation (11) can be converted into an alternative form represented by the linear and angular velocities of the UGV,

$$\begin{bmatrix} \left(m + \frac{2I_w}{r^2}\right) & 0 \\ 0 & \left(I + \frac{2L^2}{r^2} I_w\right) \end{bmatrix} \begin{bmatrix} \dot{v} \\ \dot{\omega} \end{bmatrix} + \begin{bmatrix} 0 & -m_c d\omega \\ m_c d\omega & 0 \end{bmatrix} \begin{bmatrix} v \\ \omega \end{bmatrix} = \begin{bmatrix} \frac{1}{r} & 0 \\ 0 & \frac{L}{r} \end{bmatrix} \begin{bmatrix} u_1 \\ u_2 \end{bmatrix} \tag{15}$$

where $u_1 = \tau_R + \tau_L$, $u_2 = \tau_R - \tau_L$. τ_R is right motor torque and τ_L is the left motor torque. Equation (15) is the nonlinear model of UGV. The linearised dynamic model of UGV is as follows (Mevo et al., 2018).

$$\begin{bmatrix} \left(m+\dfrac{2I_w}{r^2}\right) & 0 \\ 0 & \left(I+\dfrac{2L^2}{r^2}I_w\right) \end{bmatrix} \begin{bmatrix} \dot{v} \\ \dot{\omega} \end{bmatrix} = \begin{bmatrix} \dfrac{1}{r} & 0 \\ 0 & \dfrac{L}{r} \end{bmatrix} \begin{bmatrix} u_1 \\ u_2 \end{bmatrix} \tag{16}$$

3.3 Actuator modelling

DC motors are generally used to drive the wheels of the UGV. Armature voltage (v_a) is used as control input in DC motors and the equations of armature circuit are expressed as follows,

$$\begin{cases} v_a = R_a i_a + L_a \dfrac{di_a}{dt} + e_a \\ e_a = K_b \omega \\ \tau_m = K_t i_a \\ \tau = N\tau_m \end{cases} \tag{17}$$

where R_a is the resistance of the armature, i_a is the armature current, L_a is inductance of the armature, e_a is the back electromotive force, K_b is the back electromotive force constants, ω angular velocities of the motor, τ_m is the motor torque, K_t is the torque constant, τ is the motor torque and N is the gear ratio (Dhaouadi and Abu Hatab, 2013).

4 Controller design

4.1 Kinematic controller

The kinematic controller is used to estimate the linear and angular velocities of the UGV and is necessary for the asymptotic stability of the system. For the controller design, the position error is expressed as follows (Kanayama et al., 1990).

$$e_P = \begin{bmatrix} x_e \\ y_e \\ \theta_e \end{bmatrix} = \begin{bmatrix} \cos\theta & \sin\theta & 0 \\ -\sin\theta & \cos\theta & 0 \\ 0 & 0 & 1 \end{bmatrix} [q_r - q_A] \tag{18}$$

The kinematic-based control rule proposed by Kanayama et al. (1990) is expressed as follows,

$$\begin{bmatrix} v_c \\ \omega_c \end{bmatrix} = \begin{bmatrix} v_r \cos\theta_e + k_x x_e \\ \omega_r + v_r \left(k_y y_e + k_\theta \sin\theta_e\right) \end{bmatrix} \tag{19}$$

where k_x, k_y, k_θ are the positive gain constant.

4.2 Dynamic controller design

4.2.1 Fractional order control

The history of fractional calculus, which is an extension of full calculus dates back 300 years. In the correspondence between L'Hospital and Leibniz in 1695, the basis for fractional calculus was laid. Although its history is so old the first studies were carried out in the middle of the 19th century. It was first used in 1958 with fractional calculus controllers. With the development of technology, developments in computational systems have increased the interest in fractional control and modelling. The fractional differentiator has a general notation as in equation (20) and allows us to calculate for non-integer degrees of the derivative or integral. Fractional calculus is the use of the degree of any real number instead of the integer degree of derivative or integral expressions.

$$ {}_aD_t^r = \begin{cases} \dfrac{d^r}{dt^r} & r > 0 \\ 1 & r = 0 \\ \displaystyle\int_a^t (dt)^{-r} & r < 0 \end{cases} \tag{20} $$

In this notation a and t are the limits of the operation and $r \in R$. Grünwald-Letnikov (GL), Riemann-Louville (RL) and Caputo definitions are the most commonly used fractional differential definitions (Podlubny, 1999). These definitions are shown in equation (21) (Caponetto et al., 2010),

$$ {}_aD_t^r f(t) = \begin{cases} \lim_{h\to 0} h^{-r} \displaystyle\sum_{j=0}^{\left[\frac{t-a}{h}\right]} (-1)^j \binom{r}{j} f(t-jh) & \left[\dfrac{t-a}{h}\right] \in Z \quad GL \\ \dfrac{1}{\Gamma(n-r)} \dfrac{d^n}{dt^n} \displaystyle\int_a^t \frac{f(\tau)}{(t-\tau)^{r-n+1}} d\tau & n-1 < r < n \quad RL \\ \dfrac{1}{\Gamma(r-n)} \displaystyle\int_a^t \frac{f^n(\tau)}{(t-\tau)^{r-n+1}} d\tau & n-1 < r < n \quad Caputo \end{cases} \tag{21} $$

where for $n - 1 < r < n$, n is an integer value and $\Gamma(x)$ is the Gamma function. Since fractional order differential equations do not have exact solution methods, Laplace transforms are performed first in order to be able to solve them. The most general fractional Laplace transform notation is as in equation (22) (Na et al., 2012).

$$ L\left\{ {}_aD_t^r f(t) \right\} = s^r F(s) - \sum_{k=0}^{n-1} s^k \left[\frac{d^{m-1-k} f(t)}{dt^{m-1-k}} \right]_{t=0} \tag{22} $$

If all derivatives of the $f(x)$ function are zero, the transformation can be expressed in a simple form as follows.

$$ L\left\{ {}_aD_t^r f(t) \right\} = s^r F(s) \tag{23} $$

Then, solutions are realised by using approaches such as Carlson, Matsuda, Tustin, Simpson and Crone (Valerio and Costa, 2005). In this study, the Crone approach developed by Oustaloup and frequently used in the literature is discussed,

$$s^r = j\prod_{n=1}^{N}\frac{1+\dfrac{s}{w_{zn}}}{1+\dfrac{s}{w_{pm}}} \tag{24}$$

where $r > 0$, N is the degree of approximation, j is constant, w_{zn} and w_{pm} are the lower and upper cut off frequencies, respectively.

4.2.2 Sliding mode controller design

SMC is a robust nonlinear control method that can be easily design and applied to nonlinear systems whose parameters change over time. SMC design consists of two step. In the first step, the sliding surface is determined. The PI type sliding surface is as follows,

$$s = \begin{bmatrix} s_1 \\ s_2 \end{bmatrix} = e_c + \beta\int e_c dt \tag{25}$$

where β is a positive sliding constant, e_c is the error vector that is expressed as the difference between reference and measurement value of trajectory, e_c is expressed as follows.

$$e_c = \begin{bmatrix} e_v \\ e_\omega \end{bmatrix} = \begin{bmatrix} v_c - v \\ \omega_c - \omega \end{bmatrix} \tag{26}$$

In the second step the control signal is produced. In order to obtain the control signal (u), first the equivalent control signal (u_{eq}) and then the switching control signal (u_q) are generated. These two control signals are then summed. The general SMC law can be defined as the given below.

$$u = u_{eq} + u_d \tag{27}$$

4.2.3 Fractional order terminal sliding mode controller design

Similar processing steps apply to the FOTSMC law design. Firstly, the terminal sliding surface is defined as follows (Venkataraman and Gulati, 1993),

$$s = \dot{e}_c + \beta {e_c}^{p/q} \tag{28}$$

where p and q are both positive odd integers. The fractional order terminal sliding surface is defined as in equation (29) (Dadras and Momeni, 2012),

$$s = D^r e_c + \beta {e_c}^{p/q} \tag{29}$$

where $0 < r < 1$. In this study, the r value is determined by trial and error method. Then the control signal is obtained. For this, u_{eq} must be obtained first. Since only the u_{eq} is

valid when the system is on the sliding surface. The equivalent control signal is obtained when $s = 0$ and $\dot{s} = 0$. From equation (29), $\dot{s}$ is determined as given below,

$$\dot{s} = D^r \dot{e}_c + \beta \frac{p}{q} e_c^{(p/q)-1} \dot{e}_c \tag{30}$$

where the finite time t_s taken from $e_c \neq 0$ to $e_c(t_s) = 0$ is expressed as follows.

$$t_s = \begin{bmatrix} t_{s1} \\ t_{s2} \end{bmatrix} = \frac{1}{\beta(p-q)} e_c(t_r)^{1-(q/p)} \tag{31}$$

In equation, t_r is the time when of sliding surface reaches zero from an initial condition. In order to obtain $D^r(D^{-r}f(t)) = f(t)$ if the derivative of equation (30) is taken from order $(-r)$ and if it equals zero the following equation is obtained (Podlubny, 1999).

$$0 = \dot{e}_c + D^{-r} \beta \frac{p}{q} e_c^{(p/q)-1} \dot{e}_c \tag{32}$$

Using equation (32), the u_{eq} of the first and second controllers are obtained as follows.

$$\left.\begin{aligned} u_{eq1} &= r\left(m + \frac{2I_w}{r^2}\right)\left[\dot{v}_c + D^{-r}\beta \frac{p}{q} e_v^{(p/q)-1} \dot{e}_v\right] \\ u_{eq2} &= \frac{r}{L}\left(I + \frac{2L^2}{r^2} I_w\right)\left[\dot{\omega}_c + D^{-r}\beta \frac{p}{q} e_\omega^{(p/q)-1} \dot{e}_\omega\right] \end{aligned}\right\} \tag{33}$$

The switching control signal is as in equation (34),

$$u_d = k \operatorname{sgn}(s) \tag{34}$$

where k is a positive constant and sgn(s) is symbolic function defined by.

$$\operatorname{sgn}(s) = \begin{cases} -1 & \text{if } s < 0 \\ 0 & \text{if } s = 0 \\ 1 & \text{if } s > 0 \end{cases} \tag{35}$$

The FOTSMC signals can be rewritten as in equation (36).

$$\left.\begin{aligned} u_1 &= r\left(m + \frac{2I_w}{r^2}\right)\left[\dot{v}_c + D^{-r}\beta \frac{p}{q} e_v^{(p/q)-1} \dot{e}_v\right] + k_1 \operatorname{sgn}(s_1) \\ u_2 &= \frac{r}{L}\left(I + \frac{2L^2}{r^2} I_w\right)\left[\dot{\omega}_c + D^{-r}\beta \frac{p}{q} e_\omega^{(p/q)-1} \dot{e}_\omega\right] + k_2 \operatorname{sgn}(s_2) \end{aligned}\right\} \tag{36}$$

4.3 Stability analysis

4.3.1 Kinematic controller analysis

For Lyapunov stability, the candidate function must be positive definite and its derivative must be negative definite. The candidate L function for Lyapunov stability analysis is proposed as follows (Mevo et al., 2018).

$$L = \frac{1}{2}\left(x_e^2 + y_e^2\right) + \frac{1}{k_y}(1 - \cos\theta_e) \tag{37}$$

The time derivate of L is obtained as follows.

$$\dot{L} = \dot{x}_e x_e + \dot{y}_e y_e + \frac{1}{k_y}\left(\dot{\theta}_e \sin\theta_e\right) \tag{38}$$

Substituting the derivative of equation (18) and (19) in equation (38) the following expression is obtained.

$$\dot{L} = -k_x {x_e}^2 - \frac{v_r k_\theta \sin^2\theta_e}{k_y} \leq 0 \tag{39}$$

Consequently, so that if $v_r \geq 0$ then the $\dot{L}$ is a negative definite function. That means uniformly asymptotically stability (Mevo et al., 2018).

4.3.2 Dynamic controller analysis

The proposed candidate Lyapunov function for the first controller is as follows.

$$L_1 = \frac{1}{2}s_1^2 \tag{40}$$

The following equation is obtained by taking the derivative of equation (40).

$$\dot{L}_1 = s_1 \dot{s}_1 \tag{41}$$

If equation (30) is substituted in equation (41), the following equation can be obtained.

$$\dot{L}_1 = s_1\left[D^r \dot{e}_v + \beta\frac{p}{q}{e_v}^{(p/q)-1}\dot{e}_v\right] \tag{42}$$

If the expression $\dot{e}_v$ is substituted in equation (42) the following equation is obtained.

$$\dot{L}_1 = s_1\left[D^r\left(\dot{v}_c - \dot{v}\right) + \beta\frac{p}{q}{e_v}^{(p/q)-1}\dot{e}_v\right] \tag{43}$$

If the expression $\dot{v}$ obtained using equation (16) is substituted in equation (43) the following equation is obtained.

$$\dot{L}_1 = s_1\left[D^r\left(\dot{v}_c - \frac{u_1}{r\left(m + \frac{2I_w}{r^2}\right)}\right) + \beta\frac{p}{q}{e_v}^{(p/q)-1}\dot{e}_v\right] \tag{44}$$

If the expression u_1 in equation (36) is substituted in equation (44) the following equation is obtained.

$$\dot{L}_1 = s_1\left[D^r\left(\dot{v}_c - \left[\dot{v}_c + D^{-r}\beta\frac{p}{q}e_v^{(p/q)-1}\dot{e}_v\right] - \frac{k_1\,\mathrm{sgn}(s_1)}{r\left(m+\frac{2I_w}{r^2}\right)}\right) + \beta\frac{p}{q}e_v^{(p/q)-1}\dot{e}_v\right] \tag{45}$$

As a result, if equation (45) is rearranged, the expression given in equation (46) is obtained.

$$\dot{L}_1 = -\frac{k_1\,\mathrm{sgn}(s_1)}{r\left(m+\frac{2I_w}{r^2}\right)}s_1 < 0 \tag{46}$$

As can be seen from equation (46), if the value of k_1 is chosen positive and the candidate Lyapunov function itself is positive definite, the derivative of the Lyapunov function will be negative definite. This shows that the designed controller is stable. For the second controller, the same steps as in the first controller are applied and the expression given in equation (47) is obtained. It is seen from the equation that the second controller is also stable.

$$\dot{L}_2 = -\frac{k_2\,\mathrm{sgn}(s_2)}{\frac{r}{L}\left(I+\frac{2L^2}{r^2}I_w\right)}s_2 < 0 \tag{47}$$

5 Simulation results

In order to demonstrate the performance of the proposed controller, trapezoidal and sinusoidal signals are used as reference for linear and angular velocity, respectively. The simulation results are given in Figures 2–5. It can be seen from Figures 2 and 3 that FOTSMC follows the reference velocity faster and with lower error than TMSC and SMC. In addition, the improvements made by the proposed controller in the reference trajectory tracking error are given in Tables 1 and 2. In Table 1, the MAE results of the tracking performances of linear and angular velocities obtained using FOTSMC and SMC are given. FOTSMC appears to improve tracking error by about 13% over SMC. In Table 2, it is seen that the proposed FOTSMC approach improves the tracking error by approximately 6.146% compared to TSMC. It can also be seen from Figures 4 and 5 that the proposed controller produces control signals with smoother and lower amplitude chattering to follow reference velocities.

Table 1 Mean absolute error (MAE) for reference tracking of FOTSMC and SMC

Controllers	*The linear velocity tracking performance for trapezoidal reference*	*The angular velocity tracking performance for sinusoidal reference*
FOTSMC	0.6291	0.1255
SMC	0.7241	0.1399
Total improvement	13.119%	10.293%

Table 2 MAE for reference tracking of FOTSMC and TSMC

Controllers	*The linear velocity tracking performance for trapezoidal reference*	*The angular velocity tracking performance for sinusoidal reference*
FOTSMC	0.6291	0.1255
TSMC	0.6703	0.1279
Total improvement	6.146%	1.876%

6 Conclusions

Firstly, a kinematic controller is designed to estimate the linear and angular velocities of the vehicle. Then, a FOTSMC design is carried out to track the vehicle reference velocities. The use of the kinematic controller and the FOTSMC controller together in the control of an UGV is the novelty of this study. In the study, trapezoidal linear velocity and sinusoidal angular velocity references are chosen for the trajectory tracking control of the UGV. In order to show the performance of the proposed controller, TSMC and SMC controllers are applied to the same system and the results are compared. The simulation results show that FOTSMC is more flexible than other controllers, has lower tracking error and is more efficient as it provides good robustness and accuracy. In addition, the control signals generated by FOTSMC to follow the reference velocities are smoother compared to other controllers and chattering is negligible. As a result, it has been shown that the trajectory tracking performance of the FOTSMC method is better than other controllers.

Figure 2 The linear velocity tracking performances of controllers for trapezoidal reference (see online version for colours)

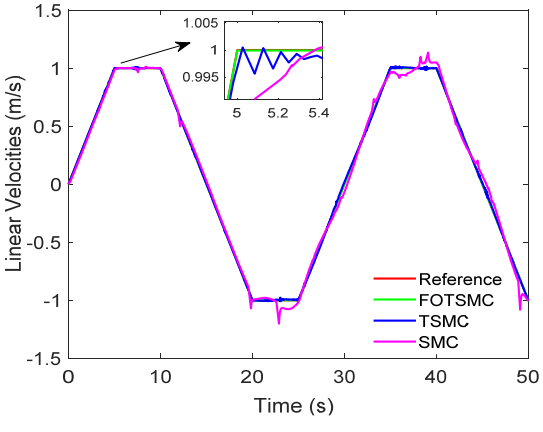

Figure 3 The angular velocity tracking performances of controllers for sinusoidal reference (see online version for colours)

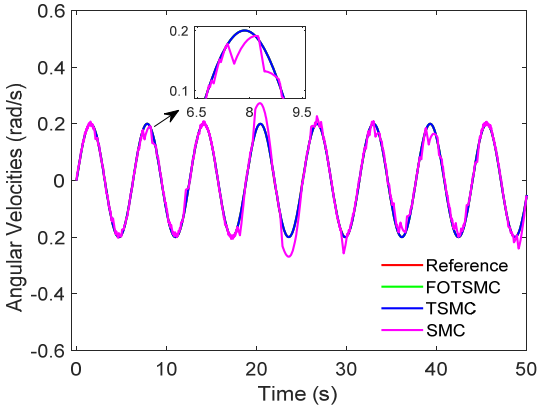

Figure 4 The control signals generated by controllers for linear velocity tracking (see online version for colours)

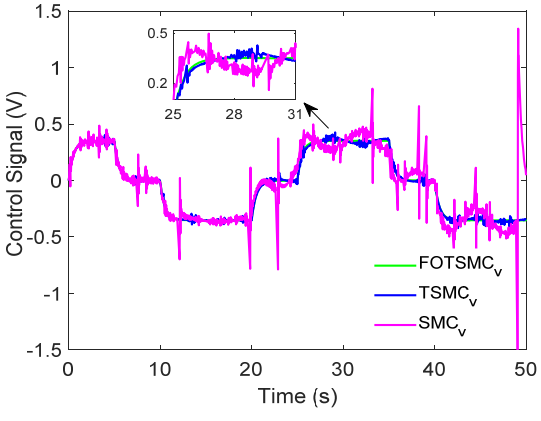

Figure 5 The control signals generated by controllers for angular velocity tracking (see online version for colours)

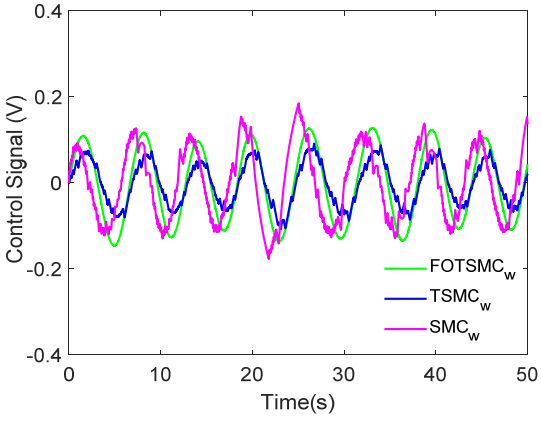

6.1 Future works

The controller proposed in this study has been tested in the simulation environment and on a vehicle with a known model. In future studies, it is desired to be tested in real-time on a vehicle with a similar configuration including disturbances and model uncertainties.

References

Asif, M., Khan, M.J. and Ning, C. (2014) 'Adaptive sliding mode dynamic controller with integrator in the loop for nonholonomic wheeled mobile robot trajectory tracking', *International Journal of Control*, Vol. 87, No. 5, pp.964–975.

Azzabi, A. and Nouri, K. (2021) 'Design of a robust tracking controller for a nonholonomic mobile robot based on sliding mode with adaptive gain', *International Journal of Advanced Robotic Systems*, Vol. 18, No. 1, pp.1–18.

Başçi, A. and Derdiyok, A. (2013) 'The application of chattering-free sliding mode controller in coupled tank liquid-level control system', *Korean J. Chem. Eng.*, Vol. 30, No. 3, pp.540–545.

Başçi, A. and Derdiyok, A. (2014) 'Real-time velocity and direction angle control of an automated guided vehicle', *International Journal of Robotics and Automation*, Vol. 29, No. 3, pp.227–233.

Başçi, A., Derdiyok, A. and Mercan, E. (2015) 'Real time fuzzy based speed and direction angle control of an automated guided vehicle', *Pamukkale University Journal of Engineering Sciences*, Vol. 21, No. 2, pp.59–65.

Can, K., Orman, K., Başçi, A. and Derdiyok, A. (2020a) 'A fractional-order sliding mode controller design for trajectory tracking control of an unmanned aerial vehicle', *Elektronika Ir Elektrotechnika*, Vol. 26, No. 4, pp.4–10.

Can, K., Sekban, H.T., Orman, K. and Başçi, A. (2020b) 'Design, simulation and comparison of controllers for temperature profile tracking control of a heat flow system', *Erzincan University Journal of Science and Technology*, Vol. 13, No. 2, pp.828–838.

Caponetto, R., Dongola, G., Fortuna, L. and Petras, I. (2010) *Fractional Order Systems: Modeling and Control Applications*, World Scientific Publ., Singapore.

Çelebi, M. and Başçi, A. (2016) 'Fractional order control of a sinusoidal output inverter', *IU-JEEE*, Vol. 16, No. 2, pp.3037–3042.

Chen, C.Y., S. Li, T.H., Yeh, Y.C. and Chang, C.C. (2009) 'Design and implementation of an adaptive sliding mode dynamic controller for wheeled mobile robots', *Mechatronics*, Vol. 19, No. 2, pp.156–166.

Dadras, S. and Momeni, H.R. (2012) 'Fractional terminal sliding mode control design for a class of dynamical systems with uncertainty', *Communications in Nonlinear Science and Numerical Simulation*, Vol. 17, No. 1, pp.367–377.

Demirbas, F. and Kalyoncu, M. (2017) 'Differential drive mobile robot trajectory tracking with using PID and kinematic based backstepping controller', *Selcuk University Journal of Engineering Science and Technology*, Vol. 5, No. 1, pp.1–15.

Dhaouadi, R. and Abu Hatab, A. (2013) 'Dynamic modelling of differential-drive mobile robots using Lagrange and Newton-Euler methodologies: a unified framework', *Advances in Robotics & Automation*, Vol. 2, No. 2, pp.1–7.

Ding, L., Li, S., Gao, H., Chen, C. and Deng, Z. (2020) 'Adaptive partial reinforcement learning neural network-based tracking control for wheeled mobile robotic systems', *IEEE Transactions on Systems, Man, and Cybernetics: Systems*, Vol. 50, No. 7, pp.2512–2523.

Fierro, R. and Lewis, F.L. (1997) 'Control of a nonholonomic mobile robot: backstepping kinematics into dynamics', *Journal Robot System*, Vol. 14, No. 3, pp.149–163.

Kanayama, Y., Kimura, Y., Miyazaki, F. and Noguchi, T. (1990) 'A stable tracking control method for an autonomous mobile robot', in *1990 IEEE International Conference*, Cincinnati, OH, USA, pp.384–389.

Koubaa, Y., Boukattaya, M. and Dammak, T. (2015) 'Adaptive sliding-mode dynamic control for path tracking of nonholonomic wheeled mobile robot', *J. Automation & Systems Engineering*, Vol. 9, No. 2, pp.119–131.

Mevo, B.B., Saad, M.R. and Fareh, R. (2018) 'Adaptive sliding mode control of wheeled mobile robot with nonlinear model and uncertainties', in *2018 IEEE Canadian Conference on Electrical & Computer Engineering*, Quebec, QC, Canada, 13–16 May, pp.1–5.

Na, G., Zhi-hong, Q. and Hai-tao, W. (2012) 'Neutral speed stability control law of aircraft design based on fractional order PiλDμ', in *2012 24th Chinese Control and Decision Conference*, Taiyuan, China, pp.2802–2805.

Orman, K., Başçi, A. and Derdiyok, A. (2016) 'Speed and direction angle control of four wheel drive skid-steered mobile robot by using fractional order PI controller', *Elektronika Ir Elektrotechnika*, Vol. 22, No. 5, pp.14–19.

Orman, K., Can, K., Başçi, A. and Derdiyok, A. (2018) 'An adaptive-fuzzy fractional-order sliding mode controller design for an unmanned vehicle', *Elektronika Ir Elektrotechnika*, Vol. 24, No. 2, pp.12–17.

Ou, M., Du, H. and Li, S. (2014) 'Finite-time formation control of multiple nonholonomic mobile robots', *International Journal of Robust and Nonlinear Control*, Vol. 24, No. 1, pp.140–165.

Oustaloup, A., Levron, F., Mathieu, B. and Nanot, F.M. (2000) 'Frequency-band complex noninteger differentiator: characterization and synthesis', *IEEE Trans CAS-I*, Vol. 47, No. 1, pp.25–39.

Podlubny, I. (1999) 'Fractional order systems and controllers', *IEEE Transactions on Automatic Control*, Vol. 44, No. 1, pp.208–214.

Sekban, H.T. and Başçi, A. (2021) 'Chattering free integral terminal sliding mode controller for trajectory tracking control of an unmanned ground vehicle', in *TOK*, Van, Turkey, 2–4 September, pp.96–101.

Sekban, H.T., Can, K. and Başçi, A. (2020) 'Model-based dynamic fractional-order sliding mode controller design for performance analysis and control of a coupled tank liquid-level system', *Advances in Electrical and Computer Engineering*, Vol. 20, No. 3, pp.93–100.

Sekban, H.T., Can, K. and Başçi, A. (2021) 'Integral terminal sliding mode controller for trajectory tracking control of unmanned ground vehicle', in *International Symposium on Applied Sciences and Engineering*, Erzurum, Turkey, 7–9 April, pp.155–160.

Sharma, A. and Panwar, V. (2016) 'Control of mobile robot for trajectory tracking by sliding mode control technique', in *2016 International Conference on Electrical, Electronics, and Optimization Techniques*, Chennai, India, 3–5 March, pp.3988–3994.

Swadi, S.M., Tawfik, M.A., Abdulwahab, E.N. and Kadhim, H.A. (2016) 'Fuzzy-backstepping controller based on optimization method for trajectory tracking of wheeled mobile robot', in *2016 UKSimAMSS 18th International Conference on Computer Modelling and Simulation*, Cambridge, UK, 6–8 April, pp.147–152.

Valerio, D. and Costa, J.S. (2005) 'Time-domain implementation of fractional order controllers. control theory and applications', *IEEE Proceedings*, Vol. 152, No. 5, pp.539–552.

Venkataraman, S.T. and Gulati, S. (1993) 'Control of nonlinear systems using terminal sliding modes', *Journal of Dynamic Systems, Measurement, and Control*, Vol. 115, No. 3, pp.554–560.

Wang, K., Liu, Y., Huang, C. and Cheng, P. (2020) 'Adaptive backstepping control with extended state observer for wheeled mobile robot', in *Proceedings of the 39th Chinese Control Conference*, Shenyang, China, 27–29 July, pp.1981–1986.

Xin, L., Wang, Q., She, J. and Li, Y. (2016) 'Robust adaptive tracking control of wheeled mobile robot', *Robotics and Autonomous Systems*, Vol. 78, pp.36–48.

Young, K.D., Utkin, V.I. and Ozguner, U. (1996) 'A control engineer's guide to sliding mode control', in *1996 IEEE International Workshop on Variable Structure Systems*, Vol. 7, No. 3, pp.1–14.

Yu, X., Feng, Y. and Man, Z. (2021) 'Terminal sliding mode control – an overview', *IEEE Open Journal of the Industrial Electronics Society*, Vol. 2, pp.36–52.